World Journal of Pharmaceutical Sciences
ISSN (Print): 2321-3310; ISSN (Online): 2321-3086
Available online at: http://www.wjpsonline.org/
Original Article

Removal of Mordant Green 17 and Acid Fast Red from Water using Nanokaolin

Sabah S. Ibrahim and Belal N.A. Mahran

Chemistry Department, Central Lab for Environmental Quality Monitoring, National Water Research Center, Elqanater Elkhayria, Egypt

Received: 14-05-2017 / Revised Accepted: 20-06-2017 / Published: 25-06-2017

ABSTRACT

Increasing concentrations of dyes including mordant green17 and acid fast RN in surface and groundwater are a major environmental concern in recent years. In this research, the potential of nanokaolin for efficient removal of MG17 and AFR residue from aqueous solutions was investigated. For this purpose, nanoKaolin was characterized by XRD, surface area and TEM techniques. Effect of various parameters such as contact time, adsorbent dosage, initial concentration of MG17 and AFR and temperature on adsorption of MG17 and AFR on nanokaolin was investigated. The results showed that the best condition for removal of MG17 and AFR was exhibited at contact time 90 min and adsorbent dosage 1g/L. the removal of MG17 and AFR decreased with the increase of initial concentration. Langmuir and Freundlich isotherm models were applied to the equilibrium data. Kinetic study applied pseudo first and second order Results indicate the potential of nanokaolin for removal of MG17 and AFR from aqueous solutions.

Keywords: Nanokaolin, Azo-dyes, Photodegradation and isotherm models

Address for Correspondence: Sabah S. Ibrahim, Chemistry Department, Central Lab for Environmental Quality Monitoring, National Water Research Center, Elqanater Elkhayria, Egypt; E-mail: sbah.ibrahim@yahoo.com

How to Cite this Article: Sabah S. Ibrahim and Belal N.A. Mahran. Removal of Mordant Green 17 and Acid Fast Red from Water using Nanokaolin World J Pharm Sci 2017; 5(7): 4-16.

INTRODUCTION

Water is an essential part of biological life and can be easily contaminated with dyes. As little as 1 ppm of dye can affect water aesthetically, and may be harmful to the environment as well as humans. Photocatalytic degradation use energy from light to excite nanoparticles to degrade dyes and produces less harmful by-products, while conventional cleaning methods produce more harmful compounds in water [1].

Waste waters containing azo-dyes are some of the most recalcitrant classes of organic compounds to treat, due to their azo groups usually attached to radicals, of which at least one is an aromatic group [2, 3]. It is well known that some azo-dyes and their degradation products are highly carcinogenic. Colored waste waters in the ecosystem are a source of aesthetic pollution, of eutrophication, and of perturbations in aquatic life [4].

A photocatalyst was obtained by treating the commercial amorphous anatase titanium dioxide with ammonia water. During the preparation of photocatalytic material the optimal conditions of the separation operation were found. The photocatalyst was characterized by UV/VIS-DR, FTIR-DR, and XRD techniques, and high-resolution transmission electron microscopy (HR-TEM). According to the XRD method, the mean crystalline size of TiO2 was 12.7-13 nm. The particulates were characterized using a particle size analyzer (mean size 195.7 nm). TEM studies presented the morphology of the sample. The photocatalytic activity of the photocatalyst was determined on the basis of the decomposition rate of phenol and azo-dye (methylene blue) under UV irradiation. The pH effects on the photocatalytic degradation were investigated [5].

TiO_2 nanoparticles have been extensively investigated for photocatalytic applications including the decomposition of organic compounds and production of H_2 as a fuel using solar energy.

The structure and electronic properties of TiO2, compares TiO2 with other common semiconductors used for photocatalytic applications and clarifies the advantages of using TiO2 nanoparticles. TiO2 is considered close to an ideal semiconductor for photocatalysis but possesses certain limitations such as poor absorption of visible radiation and rapid recombination of photogenerated electron/hole pairs [6]. The Photocatalytic degradation of methylene blue dye (MB) was studied using Titanate nanoparticles catalyst under UV light in a tubular reactor. Titanate nanoparticles were synthesized by hydrothermal reaction using TiO2 and NaOH as the precursors and calcinations at 500°C for 4 hr. The products were characterized with TEM and XRD. [7].

The scientific community is in search in for new methods for the synthesis of metallic nanoparticles. Green synthesis has now become a vast developing area of new research groups. Here we report a green method to the synthesis of silver nanoparticles (AgNPs) using the different parts of Vishanika or Indian screw tree, an ayurvedic medicinal tree. This is nontoxic, eco-friendly and low cost method. The reduction and stabilization capability of the plant extracts of different parts are described. [8].

The nanophotocatalytic process using semiconducting oxides with a nanostructure is one of the technologies used for the destructive oxidation of organic compounds such as dyes. The photocatalytic oxidation of a textile dye—C. I. Basic Blue 41 (BB41) in aqueous solution was assessed by UV ray irradiation in the presence of TiO2 nanoparticles. [9], some dyes can undergo anaerobic decolouration to form potential carcinogens [10]. The wastewater which is coloured in the presence of these dyes can block both sunlight penetration and oxygen dissolution that are essential for aquatic life. Consequently, there is a considerable need to treat these coloured effluents before discharging them into various water bodies. Various approaches on handling and decontaminating such effluents have been reported. Typical techniques include the classical methods such as adsorption [11, 12], coagulation [13, 14], ion flotation [15] and sedimentation [16].

The AgNPs were synthesized using Cordia dichotoma leaf extract and were characterized using UV-vis spectroscopy to determine the formation of AgNPs. FTIR was done to discern biomolecules responsible for reduction and capping of the synthesized nanoparticles. Further, DLS technique was performed to examine its hydrodynamic diameter, followed by SEM, TEM and XRD to determine its size, morphology and crystalline structure. Later, these AgNPs were studied for their potential role in antibacterial activity and photocatalytic degradation of azo dyes such as methylene blue and Congo red [17]. In recent years, nanotechnology has gained major acclaim in different branches of science owing to its multifaceted, beneficial properties including electrical, optical, chemical stability and catalytic activity [18, 19].

Nanoparticles of the ZnO and TiO2 were synthesized and the physicochemical properties of

the compounds were characterized by IR, X-ray diffraction (XRD), scanning electron microscopy (SEM) and transmission electron microscopy (TEM). The XRD patterns of the ZnO and TiO2 nanoparticles could be indexed to hexagonal and rutile phase, respectively. Aggregated nanoparticles of ZnO and TiO2 with spherical-like shapes were observed with particle diameter in the range of 80-100 nm. These nanoparticles were used for photocatalytic degradation of various dyes [20].

The main objective of the work is to remove different concentrations of azo-dyes from industrial waste water using photodegradation technique.

EXPERIMENTAL

Chemical and Reagents: All chemicals used in experiment were of analytical grade. Preparation of Mordant green 17 and acid fast red were at $0.5*10^{-3}$ g/L concentration. Kaolin is used at 0.1g/100ml. Apparatus: TEM spectra were recorded by JSM-6380LA scanning electron. X-ray diffraction spectra were recorded by microscope (Jeol) Altima 4 X-Ray diffraction (Rigaco).

Characterization of kaolin: The characterization of kaolin (TEM, XRD and FTR) for kaolin is discussed in figures (1, 2 and 3).
The characterization of the assessed azo-dyes is discussed in **Table: 1**

Kaolin Nanoparticles

Preparation of Kaolin Nanoparticles: Nanokaolin is a product of kaolin, also known as white clay. Kaolin was established as supplementary cementitious material in concrete. The inclusion of kaolin in concrete enhances strength and durability and prolongs concrete life span. Nanokaolin can be developed by using sol gel technique which involves high energy milling [650-750 °C]. The process of milling been influenced by time of milling, ball and jar type. Ceramic type Zirconia has been used as jar and ball type in this process. Time of milling was set from 4 hours to 24 hours. Sample was analyzed by using particle size analyzer to determine the particle size and surface area of kaolin. From the results it has been shown that the optimum milling period for nanoKaolin is 24 hours base on particle size compared to 4 hours. Furthermore, one day milling produces a massive increment of surface area compare to others. In conclusion, 24 hours could be considered as the optimum cycle time in the production of nanokaolin [21].

Batch experiments: The batch experiments were carried out in 250 ml Erlenmeyer containing 100 ml of aqueous solution. The suspension was shaken at (25 C^0) shaker at 250 rpm. The residual concentration of Mordant Green 17 and Acid Fast Red in supernatant was analysed by HACH UV-spectrophotometer. Effects of adsorbent dosage (0.1-0.4 g/L), contact time (10-60 min), initial Mordant Green 17 and Acid Fast Red concentration (0.031 to $1*10^{-3}$ g/L) and temperature (30 C^0-60 C^0) on photodegradation of Mordant Green 17 and Acid Fast Red by nanokaolin were investigated. The adsorption capacity q_e (mg/g) of the adsorbent was calculated from the following equations:

(1) $q_e = (Ci - Ce)V / W$

(2) $R\% = (Ci - Ce)\ 100 / Ci$

Where *Ci* is initial mordant green17 and acid fast red concentration, *Ce* is the residual concentration reached at equilibrium state, *V* is the volume of solution (L), R % is the removal percent and *W* is the weight of adsorbent (g).

RESULTS AND DISCUSSION

Charaterization of Kaolin Nanoparticles: A systematic characterization on kaolin has been performed by FT-IR, XRD and TEM. The FT-IR spectrum of nanokaolin is shown in **Fig. (1)**.The two absorption peaks at wavelength of 1085 cm^{-1} and 460 cm^{-1} indicats the formation of nanoparticles. **Fig. (2)** shows the powder XRD pattern of nanokaolin samples under ambient condition. The broad peak reveals the existence of an amorphous phase Kaolin .The characteristic broad peak at 12 θ to 68 θ indicates that nanoKaolin is predominately present in the sample. **Fig. (3)** shows the TEM image of fresh synthesized Kaolin of nanoparticles. It could be observed that the kaolin is in the form nanospheres, which exists in a diameter of 31- 60 nm.

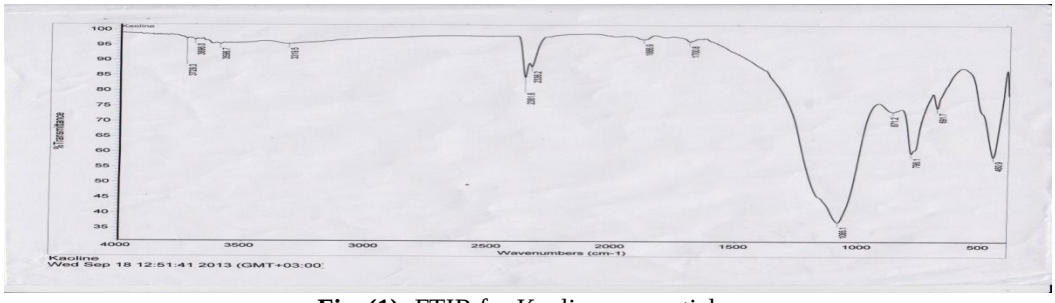

Fig. (1): FTIR for Kaolin nanoparticles

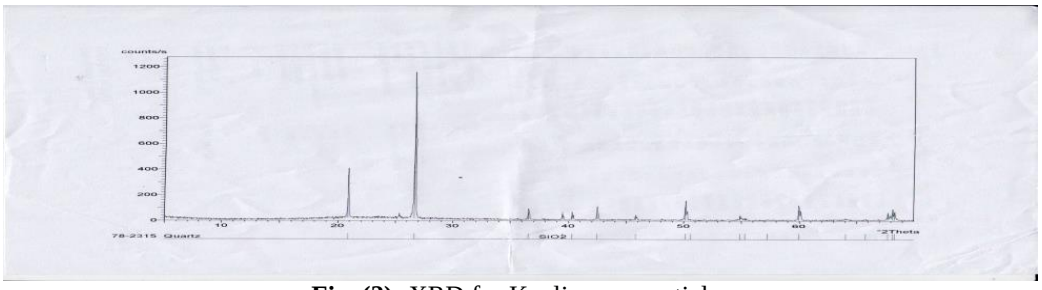

Fig. (2): XRD for Kaolin nanoparticles

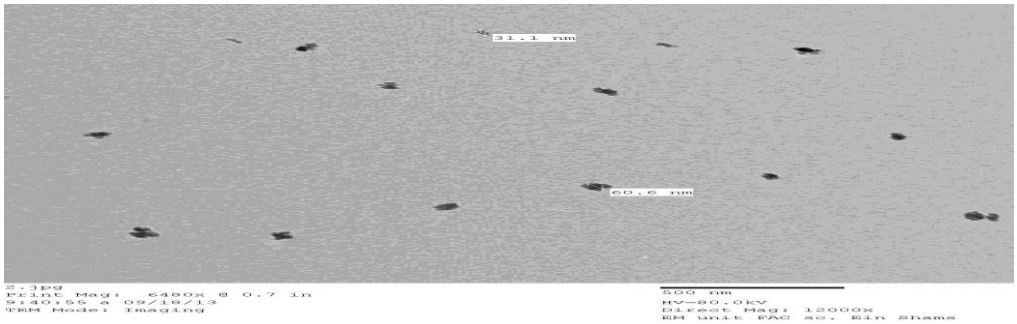

Fig. (3): TEM for Kaolin nanoparticles

Table 1: Assessed Dyes

No.	Name	Molecular Formula	Molecular Weight	Molecular Structure
D-1	**Mordant Green 17**	**$C_{16}H_{10}N_4Na_2O_{10}S_2$**	**528.38**	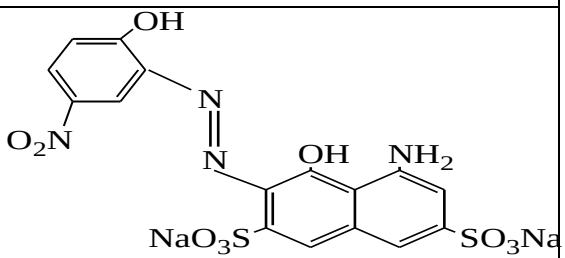
D-5	**Woodstain Scarlet "Acid Fast Red RN"**	**$C_{22}H_{14}N_4O_7S_2Na_2$**	**556.5**	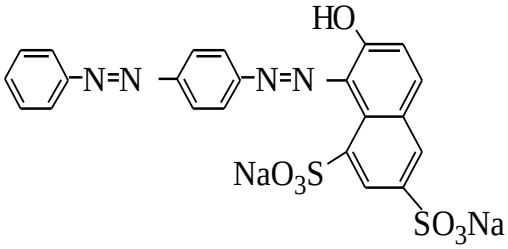

Effect of contact time in presence of UV only: During direct photolysis, photon absorption gives rise to compounds in excited electronic states that are susceptible to chemical transformation. In UV direct photolysis, the contaminant to be destroyed absorbs the incident radiation and undergoes degradation starting from its excited state [22]. UV irradiation would attack and decompose some organic molecules by bond cleavage and free radical generation, but usually at very slow rates [23]. In the presence of UV radiation, the rate of dye removal is high in the beginning indicating that degradation for dyes is fast during the first period. The removal reached its maximum value after about 15 min for AFR (80%). The percent of removal is high for MG17 (70%) at 60 min,

The mechanism of nanoTiO_2 photo catalysis is concluded as follows: TiO_2 absorbs UV light to generate electron (e^-) and hole (h^+). The holes combine with H_2O on the surface of TiO_2 to form H^+ and ·OH free radicals. H^+ and electron react to yield •H. The •H and •OH free radicals attack the organic molecule, and then produce some intermediate products. The mechanism of photo catalytic degradation under UV light irradiation is described by [24]:

$TiO_2 + h\nu \rightarrow e^- + h^+$
$h^+ + H_2O \rightarrow H^+ + \bullet OH$
$e^- + H^+ \rightarrow \bullet H$
•OH (•H) → dye → oxidative products → end product

When the dye solutions exposed to the UV radiation it is observed that photodegradation for AFR increase by increase time to reach 80% at 15 min. but in case MG17 increase photodegradation to reach 70% at 60 min. shown in **Fig(4).**

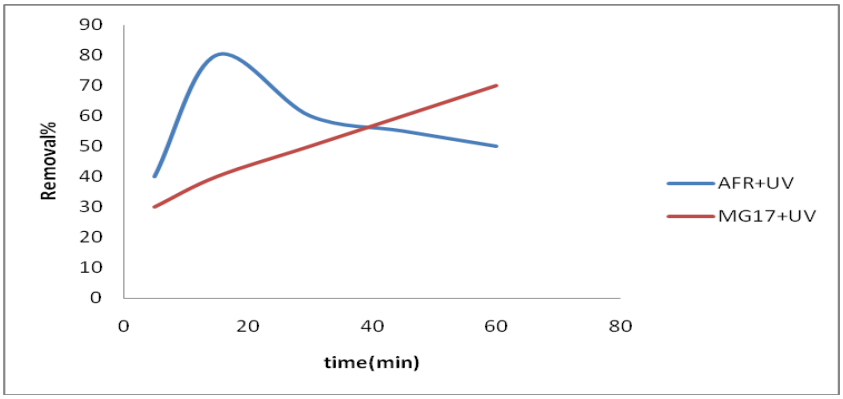

Fig. (4): Effect of contact time in present of UV only

Effect of contact time in presence of kaolin and UV lamp: When kaolin nanoparticles were used as photocatalyst in present UV lamp, the percent of MG17 removal was high and reach to (98%) at 15 min and AFR (97%) at 30 min. The experiments were performed until 60 min for all nanokaolin. The rate of removal was increase in the beginning due to a large surface area of the adsorbent that available. The relation between removal percent for two dyes under consideration and contact time is shown in **Fig.5**.

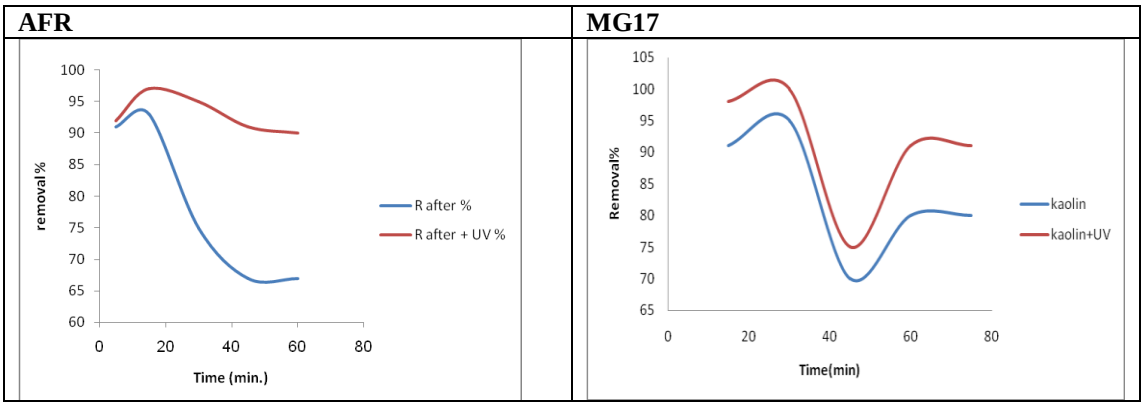

Fig. (5): Effect of contact time in present kaolin and UV lamp

Effect of different doses from nanokaolin
Fig.6, Table: 2 illustrate the effect of different amounts of nanokaolin (0. 2 to 0.4 g / 100 ml) on the removal of MG17 and AFR. It is observed that at concentration 0.2g of nanokaolin, the efficiency of removal decreased from 98% at 15 min to 90% at 60 min for AFR while MG17 efficiency of removal increased from 78% at 15 min to 97% at 60 min. Another state when using concentration 0.3 g of nanokaolin the removal % of MG17 reached 84% at 15 min but at equilibrium state, the removal % becomes 98% at 60 min and AFR reached 97% at 10 min but 90% at 60 min. Another case when using concentration 0.4 g of nanokaolin removal % reached 85% at 15 min and 99% at equilibrium state for MG17 and AFR reached to 93% at 10 min and 85 % at 60 min at equilibrium state.

Table 2: Effect of different dose

Azo-Dye	Time (min.)	Conc. (gm)		
		0.2	**0.3**	**0.4**
AFR	15	98	97	93
	60	90	90	85
MG17	15	78	84	85
	60	97	98	99

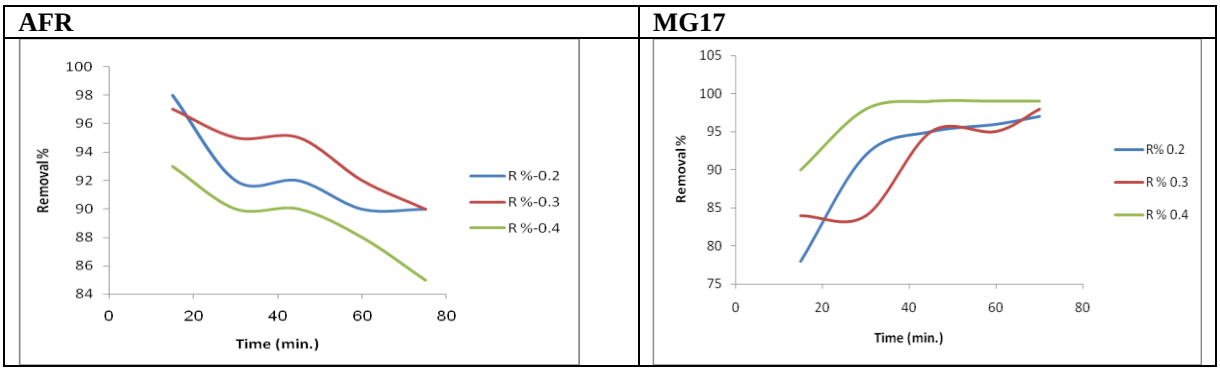

Fig. (6): Effect of different dose from nanokaolin

Effect of Initial Dye Concentration on Dye Uptake: The dye uptake mechanism is particularly dependent on the initial dye concentration: at low concentrations, dyes are adsorbed by specific sites, while with increasing dyes concentrations from ($0.25*10^{-3}$ to $1*10^{-3}$) the specific sites are saturated and the exchange sites are filled. It is observed that with increasing initial concentrations, the adsorption capacity increases while the percent dyes removal decreases. Though an increase in dye uptake was observed, the decrease in percentage adsorption may be attributed to lack of sufficient surface area to accommodate much more dyes available in the solution. At lower concentrations, the dye present in solution could interact with the binding sites and thus the percentage adsorption was higher [24]. The general shapes of the isotherms are similar for different biomasses. However, the adsorption capacities and affinities are significantly different. In the same time, literature showed that adsorption is independent of the contaminant concentration, and in some cases, the rate is lowered with increased initial concentration [25]. Different explanations were proposed, all of which rely on the adsorption of contaminant molecules on the solid surface. One explanation assumed that at high contaminant concentration, the contaminant molecules may compete with the adsorbed intermediates and inhibit degradation [26].

Effect of dye concentrations removal by nano kaolin in present UV lamp: The effect of initial dyes concentration on the rate of dyes uptake onto nanokaolin was studied using batch agitation in 250 ml beakers containing dye solutions of initial concentrations ranging from $1*10^{-3}$ to 0.031 mg L^{-1}, agitated at 250 rpm and at room temperature (25±1°C) without any change in the initial pH of the test solution. The equilibrium concentration was evaluated after 75 min of contact time. The photo degradation for dye data presented in **Fig (7)** indicates that the percentage removal of MG17 and AFR decreases with increase in initial MG17 and AFR concentration. Explain the effect of UV lamp making photo degradation for MG 17 and AFR to reach maximum removal% reach to 97% for AFR at 30 min and MG17 reach to 98% at 15 min at best concentration for dye $0.5*10^{-3}$.

Effect of pH in photo degradation of MG17 and AFR in present UV lamp: Effect of pH on photodegradation of MG17 and AFR on surface of nanokaolin are variable, but give maximum degradation at natural pH =3 for AFR 98% and MG17 reach removal 100% at pH =3 and 4 in **Fig.(8).**

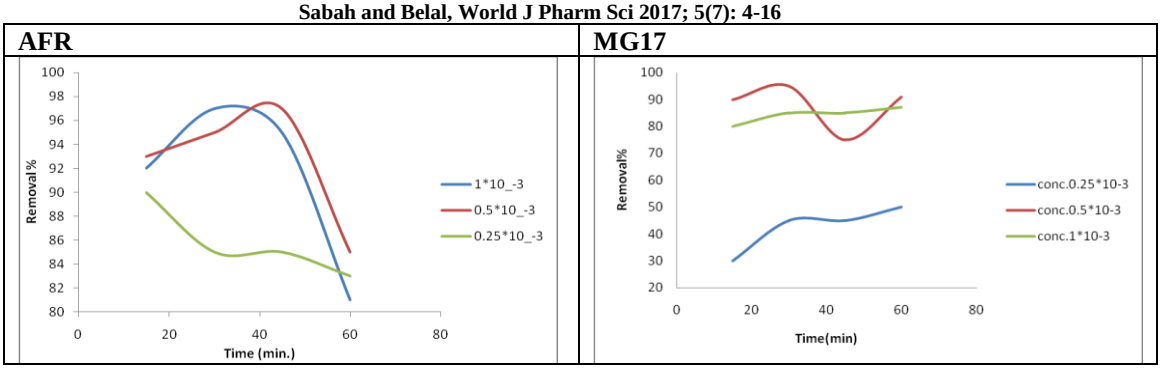

Fig. (7): Effect of dyes concentration removal by nano kaolin in present UV lamp

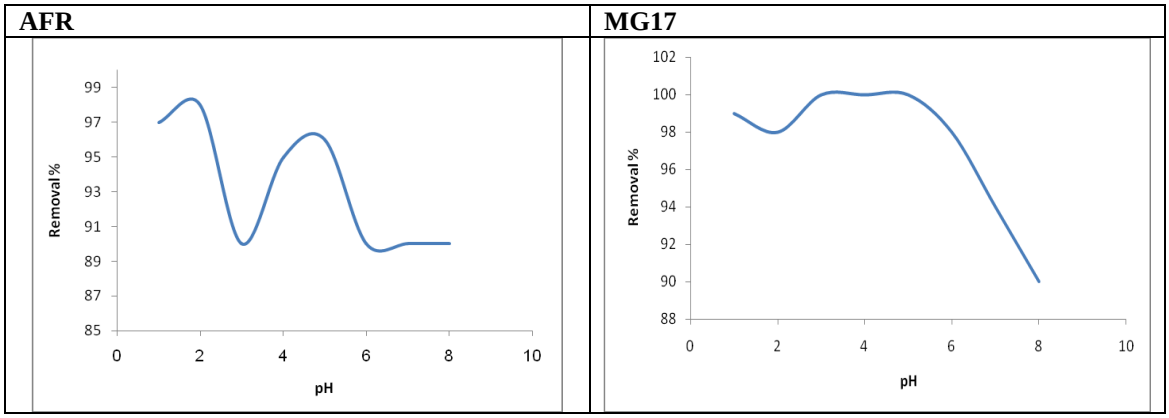

Fig.(8): Effect of pH in photo degradation of MG17 and AFR in present UV lamp

Effect of temperature for removal of AFR and MG17 in presence of UV lamp: The temperature of the medium could be important for energy-dependent mechanisms in the removal efficiency by different materials. The reason of this effect is thought to be the fact that temperature is an important factor affecting the adsorption and photo catalysis. In the case of photo catalytic process, the photo catalytic degradation rate decreases with increasing temperature. In other words, higher temperature provides higher electron transfers in valance bond to higher energy levels and hence facilitating the electron-hole production that could be utilized in initiating oxidation and reduction reactions [27]. The species photon-generated holes, and electrons, and hydroxyl radicals (•OH) can thus degrade organic pollutant to intermediates, and then the intermediates are further degraded to CO_2 and H_2O. In general, the activated energy of photo catalytic reaction is slightly affected by the temperature, but consecutive redox reaction may be largely influenced by temperature which affects both collision frequency of molecules and adsorption equilibrium [28]. So the overall effect on the photo catalytic performance will depend on the relative importance of these phenomena. AFR removal% decrease from 90% at 40ºc to 73 at 60ºc but in MG17 removal% decrease from 98% at 40ºc to 73 at 60ºc.

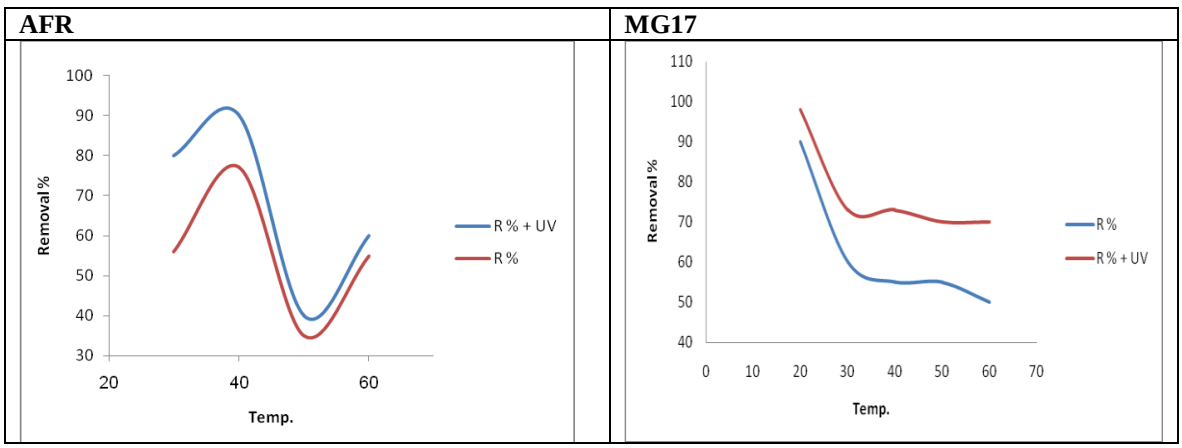

Fig.(9): Effect of temperature for removal MG17 and AFR in presence of UV lamp

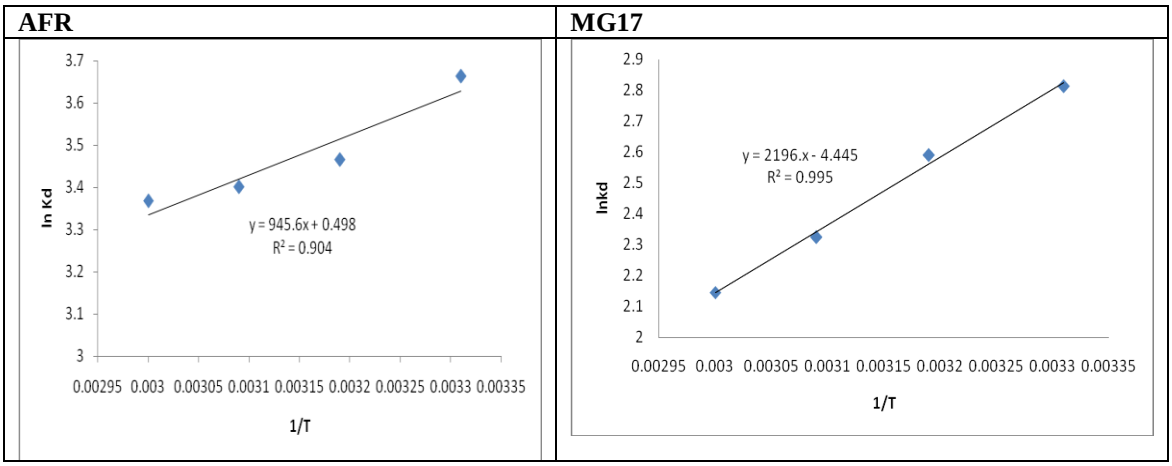

Fig. (10): Effect of temperature on removal MG17 and AFR by using nanokaolin

In order to evaluate the thermodynamic feasibility of the removal process and to confirm the nature of the adsorption process, thermodynamic parameters (ΔG^o, ΔH^o and ΔS^o) were calculated from the following equations [5,6]:

$$K_D = \frac{C_{Ad}}{C_e} \quad (4)$$

$$\Delta G = -RT\ lnK_D \quad (5)$$

$$lnK_D = -\left(\frac{\Delta H}{RT}\right) + \frac{\Delta S}{R} \quad (6)$$

where K_D is the equilibrium constant, C_{Ad} (mg/L) is the concentration of the dye adsorbed on solid at equilibrium, C_e (mg/L) is the equilibrium concentration of dye in the solution, R is the universal gas constant, 8.314 J/mol^{-1}/K, T is the absolute temperature in K, and the value of K_D in can be obtained from the adsorption percent at equilibrium. The values of ΔH and ΔS can be obtained from the slope and intercept of a van't Hoff plot of ln K_D versus 1/T as seen in Fig 10. and the thermodynamic parameters for adsorption of DGB and MO37 on kaolin are listed in Tables 4, 6.

Table 3: Effect of temperature on removal for MG17

T	1/T	Removal%	K_D	ln K_D	R^2
303	3.30x10^{-3}	98	16.66	2.813011	0.995
313	3.195x10^{-3}	73	13.33	2.590017	intercept = -4.44496
323	3.096x10^{-3}	73	10.22	2.324347	
333	3.003x10^{-3}	73	8.55	2.145931	slope = 2196.437

Table 4: Thermodynamic parameters for MG17

ΔH kJ/mol	ΔS J/mol	ΔG kJ/mol			
		303 k	313 k	323 k	333 k
-18261.2	-36.955	-7.086	-6.739	-6.067	-5.780

Table 5: Effect of temperature on removal for AFR

T	1/T	Removal%	K_D	ln K_D	R^2
303	3.30x10^{-3}	80	39	3.663562	0.904
313	3.195x10^{-3}	90	32	3.465736	Intercept= 0.498129
323	3.096x10^{-3}	70	30	3.401197	Slope = 945.6135
333	3.003x10^{-3}	60	29	3.367296	

Table 6: Thermodynamic parameters for AFR

ΔH kJ/mol	ΔS J/mol	ΔG kJ/mol			
		303 k	313 k	323 k	333 k
-7861.8	4.141446	-9.229	-9.018	-8.879	-9.070

Adsorption Isotherms: The adsorption isotherm indicates how the adsorption molecules distribute between the liquid phase and the solid phase when the adsorption process reaches an equilibrium state. The analysis of the isotherm data by fitting them to different isotherm models is an important step to find the suitable model that can be used for design purpose. The isotherm data were fitted to the Langmuir and Freundlich isotherms.

The Langmuir Model: The Langmuir adsorption isotherm has been successfully applied to many pollutants adsorption processes and has been the most widely used sorption isotherm for the sorption of a solute from a liquid solution [29]. The saturated monolayer isotherm can be represented as:

$$q_e = \frac{Q_0 b C_e}{1 + bC_e}$$

The above equation can be rearranged to the common linear form:

$$\frac{C_e}{q_e} = \frac{1}{Q_0 b} + \frac{C_e}{Q_0}$$

Where C_e is the equilibrium concentration (mg/L); q_e is the amount of dye adsorbed per unit mass of adsorbent (mg/g); Q_0 is q_e for a complete monolayer (mg/g), a constant related to sorption capacity; and b is a constant related to the affinity of the binding sites and energy of adsorption (L/mg). A high b value indicates a high affinity. The values of Q_0 and b were for all adsorbents determined respectively from intercept and slopes of the linear plots of C_e/q_e vs. C_e.

The essential characteristics of Langmuir isotherm can be expressed by a dimensionless constant called equilibrium parameter R_L, defined by [30]:

$$R_L = lnK_F + \frac{1}{n} lnC_e$$

The value of R_L indicates the type of the isotherm to be either unfavorable ($R_L > 1$), linear ($R_L = 1$), favorable ($0 < R_L < 1$) or irreversible ($R_L = 0$).

Langmuir Adsorption Isotherm for nanokaolin: The different adsorption parameters for adsorption of MG17 and AFR are collected in **Table 6**. These parameters are C_0, C_e, ln C_e, q_e, ln q_e and C_e/q_e. The plot of C_e vs. C_e/q_e gave straight lines for all dyes **Fig. (**11), from their slopes and intercepts, the values of Q_0 and b could be evaluated, respectively. The data obtained for slope, intercept, Q_0 and b are shown in **Table 9**. The applicability of the model was examined by evaluating the correlation coefficient (R). The higher the values of R, the more applicable the model for the dye examined.

Table 7: Adsorption parameters for MG17 on nanokaolin.

Azo-Dye	C_0	C_e	$ln\ C_e$	q_e	$ln\ q_e$	C_e/q_e
MG17	0.001	1.58E-04	-8.7558	0.00021	-8.465	7.50E-01
	0.005	7.11E-04	-7.2495	0.0010	-6.8378	6.63E-01
	0.0001	1.00E-03	-6.9076	-0.0002	-6.5254	-4.44E+0
	0.00006	8.00E-05	-9.872	-5E-06	-12.127	-1.60E+0
	0.00003	2.00E-05	-10.898	2.5E-06	-12.899	8.00E+0

Table 8: Adsorption parameters for AFR on nanokaolin.

Azo-Dye	C_0	C_e	$ln\ C_e$	q_e	$ln\ q_e$	C_e/q_e
AFR	0.001	0.00020	-8.4942	0.000318147	-8.053	0.6432038
	0.005	0.00078	-7.1479	0.001685393	-6.3857	0.4666666
	0.002	0.00038	-7.8728	0.000647619	-7.3422	0.5882352
	0.0001	2.14E-05	-10.750	3.14286E-05	-10.367	0.6818181
	0.00006	2.03E-05	-10.803	1.5871E-05	-11.051	1.2804878
	0.00003	8.23E-06	-11.708	8.70968E-06	-11.651	0.9444444

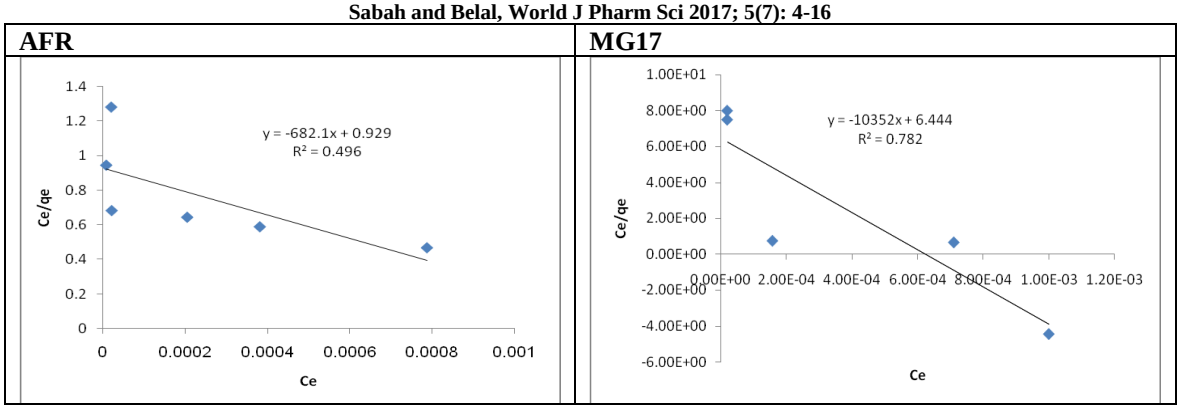

Fig. (11): Langmuir isotherm for MG17 and AFR with nanokaolin.

Table 9: Langmuir equation parameters for nanokaolin.

Azo-Dye	Slope	Intercept	Q_0	b	R^2
MG17	-10352.2	6.444884	9.6*10-5	0.005	0.782
AFR	-682.131	0.9291501	0.0014	0.001	0.496

The Freundlich Model: On the other hand, the Freundlich isotherm assumes that the adsorption occurs on heterogeneous surface at sites with different energy of adsorption and with non-identical adsorption sites that are not always available. Mathematically it is characterized by the heterogeneity factor '1/*n*'[31]. Freundlich model can be represented by the linear form as follows:

$$lnq_e = \ln K_F + \frac{1}{n} lnC_e$$

where K_F is the Freundlich constant (mg/g)/(L/mg)^n and n is the heterogeneity factor. The K_F value is related to the adsorption capacity; while 1/n value is related to the adsorption intensity. A plot of $ln\ q_e$ versus $ln\ C_e$, gives a straight line with K_F and 1/n determined from the intercept and the slope, respectively.

Freundlich Adsorption Isotherm for nanokaolin: The adsorption isotherm was applied for adsorption of different dyes on nanokaolin by drawing the relation between ln C_e and ln q_e Fig**. (12)** The slope of the resulting straight line is equals to 1/n, while the intercept equals to $ln\ K_F$. The data obtained for Freundlich isotherm model for AFR and MG17 are collected in **Tables 7 and 8**. The calculated Freundlich isotherm constants and the corresponding coefficient of correlation values are shown in **Table 10**. The coefficient of correlation was high (R^2 values are 0.990 and 0.951) indicating a good linearity. The results show that the values of n are greater than unity (n) indicating that dye is favorably adsorbed on MG17 and AFR of Freundlich constants indicate easy uptake of dyes from aqueous solution.

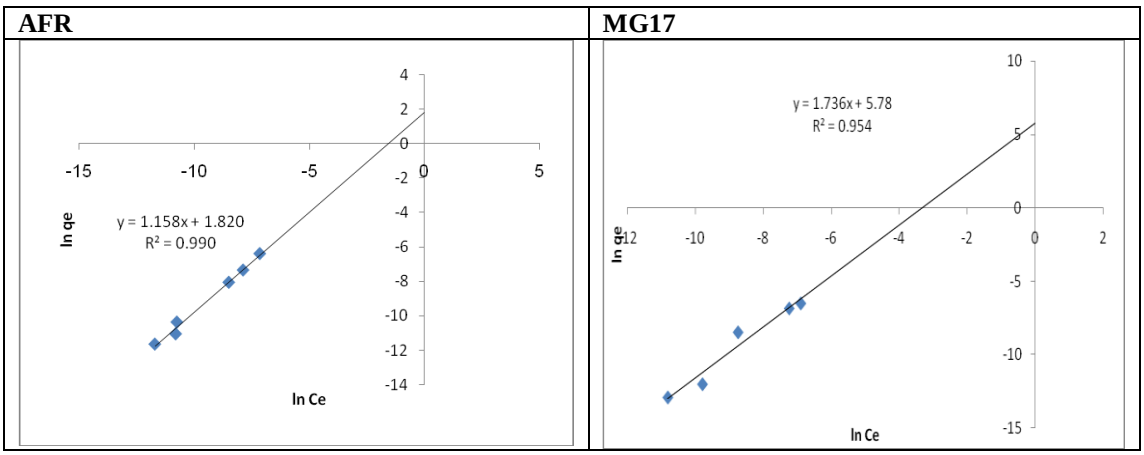

Fig. (12): Freundlich isotherm AFR and MG17 on nanokaolin

Table 10: Freundlich equation parameters for nano kaolin.

Azo-Dye	Slope	Intercept	K_F	*n*	R^2
MG17	1.728417	5.733205	308.958	-1.112E-05	0.959
AFR	1.158486	1.820913	6.177493	-2.1E-05	0.990

Kinetic Studies: The pseudo-first order equation is generally expressed as follows [32]:

$$\log(q_e - q_t) = \log q_e - (\frac{k_1}{2.303})t$$

where q_e and q_t are the sorption capacities at equilibrium and at time *t*, respectively (mg g^{-1}) and k_1 (min^{-1}) is the rate constant. The equation applicable to experimental results generally differs from a true first order equation in two ways: (i) the parameter log (q_e–q_t) does not represent the number of available sites and (ii) the parameter log (*q*e) is an adjustable parameter and often it is found not equal to the intercept of a plot of log (*q*e–*qt*) against *t*, whereas in a true first order log (q_e) should be equal to the intercept of a plot of log (q_e–q_t) against *t*. In order to fit the pseudo-first order equation to experimental data, the equilibrium capacity, q_e must be known.

On the other hand, if the rate of degradation is a second-order mechanism, the pseudo-second order kinetic rate equation is expressed as:

$$\frac{t}{q_t} = \frac{1}{k_2 q_e^2} + \frac{1}{q_e}t$$

Where *q*e and *qt* are the sorption capacities at equilibrium and at time *t*, respectively (mg g^{-1}) and *k* is the rate constant of pseudo-second order reaction (g mg^{-1} min^{-1}).

If pseudo-second-order kinetics are applicable, the plot of t/q_t against *t* should give a linear relationship, from which *q*e and k_2 can be determined from the slope and intercept of the plot.

Table 11: Photodegardation parameters of dyes on nano kaolin.

Dyes	Log (q_e-q_t)	T (min)
MG17	-0.193 -0.124 -0.123 -2.397	15 30 45 60
AFR	-0.484 -0.460 -0.469 -0.494	15 30 45 60

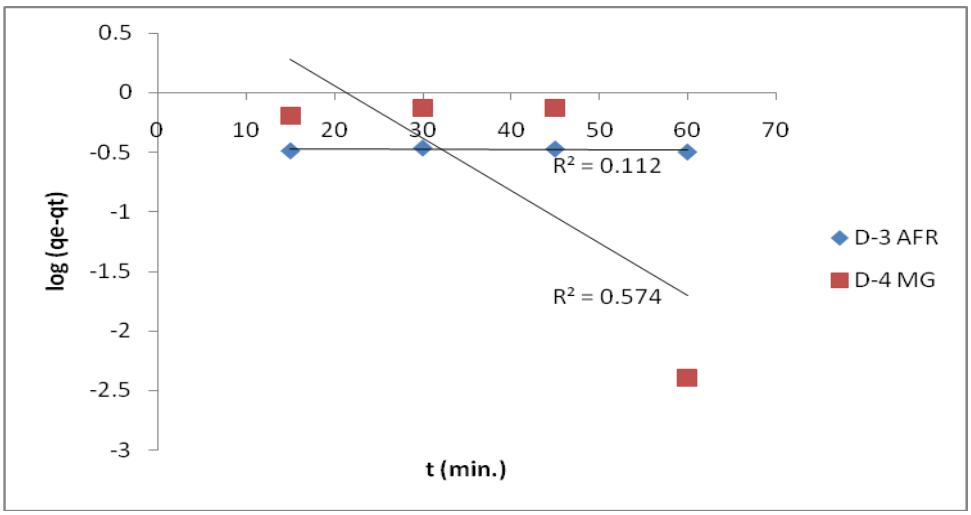

Fig. (13): The pseudo-first order for AFR and MG17 on nanokaolin

Table 12: Photodegardation parameters of dyes on nano kaolin.

Dyes	t/qt	T(min)
MG17	23.43 39.89 59.8 79	15 30 45 60
AFR	45.73 86.2 132.3 187	5 30 45 60

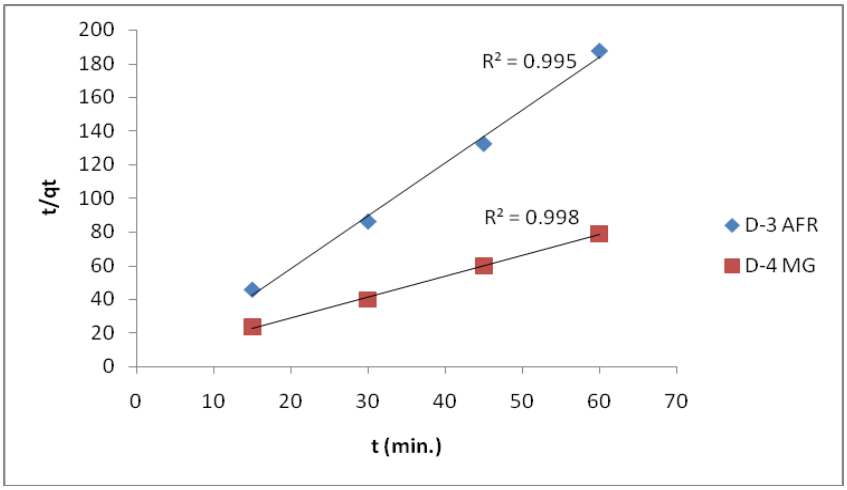

Fig. (13): The pseudo-secand order for AFR and MG17 on nanokaolin

CONCLUSION

Heterogeneous photocatalysis using kaolin nanoparticles as photocatalyst was proven to be an effective method for the degradation of AFR and MG17 in its aqueous solution. The experimental results demonstrated that increasing the substrate concentration, light exposure period, and kaolin dosage in an appropriate range contributed to the photocatalytic degradation of AFR and MG17. The removal of the dyes by adsorption on kaolin nanoparticles was found to follow Fresundlich isotherm model. The rate of photodegradation follows second order with a rate constant -2.1015 and 0.3994 min^{-1} for AFR and MG17 respectively.

REFERENCE

1. Kankeu E., Waanders F., Geldenhuys M., Photocatalytic Degradation of Dyes using TiO2Nanoparticles of Different Shapes, 7th International Conference on Latest Trends in Engineering & Technology. 2015; (ICLTET'2015) Nov. 26-27, Irene, Pretoria (South Africa).
2. Tang WZ., AN H., UV/TiO2 photocatalytic oxidation of commercial dyes in aqueous solutions. Chemosphere 1995; (31) 4157.
3. Mohapatra P., Parida KM., Photocatalytic activity of sulfate modified titania 3: Decolorization of methylene blue in aqueous solution. J. Mol. Catal. A: Chemical 2006; (258) 118.
4. Lachheb H., Puzenat E., Houas A., Ksibi M., Photocatalytic degradation of various types of dyes (Alizarin S, Crocein Orange G, Methyl Red, Congo Red, Methylene Blue) in water by UV-irradiated titania. Appl. Catal. B: Environmental 2002; (39) 75.
5. Bubacz K., Choina J., Dolat D., Morawski AW., Methylene Blue and Phenol Photocatalytic Degradation on Nanoparticles of Anatase TiO2, Polish J. of Environ. Stud. 2010; (19) 4: 685-691 .
6. Mital GS., Manoj T. A review of TiO2 nanoparticles, Chinese Science Bulletin 2011; (56) 16: 1639–1657.

7. Tayeb MA., Hussein SD. Synthesis of TiO2Nanoparticles and Their Photocatalytic Activity for Methylene Blue, Am J Nanomater. 2015; (3) 2: 57-63.
8. Bhakya S., Muthukrishnan S., Sukumaran M., Muthukumar, Catalytic Degradation of Organic Dyes using Synthesized Silver Nanoparticles: A Green Approach, Bioremediation & Biodegradation 2015; 6:5.
9. Giwa A., Nkeonye PO., Bello KA., Ademola K., Photocatalytic Decolourization and Degradation of C. I. Basic Blue 41 Using TiO2 Nanoparticles, *J Environ Protec.* 2012; 3: 1063-1069.
10. Alam M Z., Ahmad S., Malik A. and Ahmad M., Mut- agenicity and Genotoxicity of Tannery Effluents Used for Irrigation at Kanpur, India, *Ecotox Environ Safety* 2010; (73) 7: 1620-1628.
11. Nasuha N., Hameed BH. and Din ATM., Rejected Tea as a Potential Low-Cost Adsorbent for the Removal of Methylene Blue, *J Hazard Mater* 2010: (175) 1-3: 126-132.
12. Rauf MA., Qadri SM., Ashraf S. and Al-Mansoori KM., Adsorption Studies of Toluidine Blue from Aqueous So- lutions onto Gypsum, *Chem Eng J.* 2009; (150) 1: 90-95.
13. Ahmad AL. and Puasa SW., Reactive Dyes Decolouri- zation from an Aqueous Solution by Combined Coagula- tion/Micellar-Enhanced Ultrafiltration Process, *Chem Eng J.* 2007; (132) 1-3: 257- 265.
14. Riera-Torres M., Gutiérrez-Bouzán C. and Crespi M., Combination of Coagulation-Flocculation and Nanofiltration Techniques for Dye Removal and Water Reuse in Textile Effluents, *Desalination* 2010; (252) 1-3: 53- 59.
15. Shakir K., Elkafrawy AF., Ghoneimy HF., Elrab SG. and Refaat M., Removal of Rhodamine B (A Basic Dye) and Thoron (an Acidic Dye) from Dilute Aqueous Solutions and Wastewater Simulants by Ion Flotation, *Water Res.* 2010; (44) 5: 1449-1461.
16. Zodi S., Potier O., Lapicque F. and Leclerc JP., Treatment of the Industrial Wastewaters by Electrocoagulation: Optimization of Coupled Electrochemical and Sedimentation Processes, *Desalination* 2010; (261) 1-2: 186-190.
17. Mankamna R., Thapa N., Gupta N., Kumar A., Antibacterial and photocatalytic degradationefficacy of silver nanoparticles biosynthesized using Cordia dichotoma leafextract, Advances in Natural Sciences: Nanoscience and Nanotechnology 2016; 7.
18. Pulit J., Banach M . and Kowalski Z.E col Chem Eng 2011; (18) 185
19. Vaidyanathan R., Kalishwaralal K., Gopalram S., Gurunathan S., Biotechnol. Adv 2009.
20. Aminia M., Ashrafia M., Photocatalytic degradation of some organic dyes under solar light irradiation using TiO2 and ZnO nanoparticles, Nano. Chem. Res., 2016; (1) 1: 79-86.
21. Zhang XW., Zou G., Li S., Liu X., Determination of selected antibiotics in the Victoria Harbour and the Pearl River, South China using high-performance liquid chromatography–electrospray ionization tandem mass spectrometry. Environ. Pollut. 2007; 145: 672–679.
22. Kolpin D.W., Furlong E.T., Meyer MT., Pharmaceuticals, hormones and other organic wastewater contaminants in US streams, a national reconnaissance. Environ. Sci. Technol. 2000; 36: 1202–1211.
23. Kim S.C., Carlson K., Temporal and spatial trends in the occurrence of human and veterinary antibiotics in aqueous and river sediment matrices. Environ. Sci. Technol. 2007; 41: 50–57.
24. Kummerer K., Significance of antibiotics in the environment. J.J. Antimicrob. Chemother. 2003; 52: 5‑7.
25. Levy SB., Chadwick DJ., Goode FE., Antibiotic resistance: an ecological imbalance. In Antibiotic Resistance: Origins, Evolution, Selection and Spread; Wiley: Chichester. 1997: 1‑14.
26. Baquero F., Negri MC., Morosini MI., Blazquez J., The antibiotic selective process: concentration-specific amplification of lowlevel resistant populations. In Antibiotic Resistance: Origins, Evolution, Selection and Spread; Wiley: Chichester. 1997; 93‑105.
27. Loke M. , Tjornelund J. , Halling-Sorensen B., Determination of the distribution coefficient (log K_d) of oxytetracycline, tylosin a, olaquindox, and metronidazole in manure. Chemosphere, 2002; 48: 351‑361.
28. Chopra I., Roberts M., Tetracycline antibiotics: mode of action, applications, molecular biology, and epidemiology of bacterial resistance. Microbiol Mol. Biochem. Parasitol. 2001; 65: 232‑260.
29. Berger T., Sterrer M., Diwald O., Kno1zinger E., Panayotov D., Thompson TL., Yates JT., Light-induced charge separation in anatase TiO_2 particles, J. Phys. Chem. 2005; 109: 6061–6068.
30. Li FB., Li XZ., Hou MF., Cheah KW., Choy WC., Enhanced photocatalytic activity of Ce^{3+}–TiO_2 for 2-mercaptobenzothiazole degradation in aqueous suspension for odour control, Appl. Catal., 2005; 285: 181–189.
31. Norhasri MS., Hamidah MS., Abd Halim AG., Zil AM., Sol Gel Characterization of Nano Kaoline, Adv. Mater. Res, 2014; 856: 285-289.
32. Chern JM., Wu CY., Desorption of dye from activated carbon beds: effects of temperature, pH and alcohol, Water. Res. 2001; 35 : 4159–4165.